Atmos. Chem. Phys. Discuss., 9, 10957–11004, 2009
www.atmos-chem-phys-discuss.net/9/10957/2009/

Atmospheric Chemistry and Physics Discussions

This discussion paper is/has been under review for the journal *Atmospheric Chemistry and Physics (ACP)*. Please refer to the corresponding final paper in *ACP* if available.

Parameterizing the competition between homogeneous and heterogeneous freezing in ice cloud formation – polydisperse ice nuclei

D. Barahona[1] **and A. Nenes**[1,2]

[1]School of Chemical and Biomolecular Engineering, Georgia Institute of Technology, GA, USA
[2]School of Earth and Atmospheric Sciences, Georgia Institute of Technology, GA, USA

Received: 29 March 2009 – Accepted: 22 April 2009 – Published: 5 May 2009

Correspondence to: A. Nenes (athanasios.nenes@gatech.edu)

Published by Copernicus Publications on behalf of the European Geosciences Union.

Abstract

This study presents a comprehensive ice cloud formation parameterization that computes the ice crystal number, size distribution, and maximum supersaturation from precursor aerosol and ice nuclei with any size distribution and chemical composition. The parameterization provides an analytical solution of the cloud parcel model equations and accounts for the competition effects between homogeneous and heterogeneous freezing, and, between heterogeneous freezing in different modes. The diversity of heterogeneous nuclei is described through a nucleation spectrum function which is allowed to follow any form (i.e., derived from classical nucleation theory or from empirical observations). The parameterization reproduced the predictions of a detailed numerical parcel model over a wide range of conditions, and several expressions for the nucleation spectrum. The average error in ice crystal number concentration was −2.0±8.5% for conditions of pure heterogeneous freezing, and, 4.7±21% when both homogeneous and heterogeneous freezing were active. Apart from its rigor, excellent performance and versatility, the formulation is extremely fast and free from requirements of numerical integration.

1 Introduction

Ice clouds play a key role in rain production (e.g., Lau and Wu, 2003), heterogeneous chemistry (e.g., Peter, 1997), stratospheric water vapor circulation (e.g., Hartmann et al., 2001), and the radiative balance of the Earth (Liou, 1986). Representation of ice clouds in climate and weather prediction models remains a challenge due to the limited understanding of ice cloud formation processes (e.g., Lin et al., 2002; Baker and Peter, 2008), and the challenges associated with in-situ observations and remote sensing (Waliser et al., 2009). Anthropogenic activities can potentially influence ice cloud formation and evolution by altering the concentration and composition of precursor aerosols (Seinfeld, 1998; Penner et al., 1999; Minnis, 2004; Kärcher et al., 2007),

ACPD

9, 10957–11004, 2009

which may result in a potentially important indirect effect (e.g., Kärcher and Lohmann, 2003), the sign and magnitude of which is highly uncertain.

Ice clouds form by homogeneous freezing of liquid droplets or heterogeneous freezing upon ice nuclei, (IN) (e.g., Pruppacher and Klett, 1997). Observational data show that the two freezing mechanisms are likely to interact during cloud formation (DeMott et al., 2003a, b; Haag et al., 2003b; Prenni et al., 2007); their relative contribution is however a strong function of IN and droplet concentration, and cloud formation conditions (Gierens, 2003; Kärcher et al., 2006; Barahona and Nenes, 2009). The primary interaction between the freezing of IN and liquid droplets occurs through the gas phase (DeMott et al., 1997; Kärcher et al., 2006; Barahona and Nenes, 2009); IN tend to freeze early during cloud formation, depleting water vapor supersaturation and hindering the freezing of IN with high freezing thresholds and the homogeneous freezing of liquid droplets (e.g., DeMott et al., 1997; Koop et al., 2000). Although numerous aerosol species have been identified as active IN, dust, soot, and organic particles are thought to be the most relevant for the atmosphere (DeMott et al., 2003a; Sassen et al., 2003; Archuleta et al., 2005; Möhler et al., 2005; Field et al., 2006; Kanji et al., 2008; Phillips et al., 2008). Assessment of the indirect effect resulting from perturbations in the background concentration of IN requires a proper characterization of the spatial distribution of potential IN species and their freezing efficiencies (i.e., the aerosol freezing fraction). The large uncertainty in ice cloud indirect forcing is associated with incomplete understanding of these factors which is evident by the large predictive uncertainty of aerosol-cloud parameterizations (Phillips et al., 2008; Eidhammer et al., 2009).

Several approaches have been proposed to parameterize ice cloud formation in atmospheric models. Empirical correlations derived from field campaigns are most often employed to express IN concentrations (e.g., Meyers et al., 1992; DeMott et al., 1998) as a function of temperature, T, and supersaturation over ice, s_i. These expressions are simple but only provide the availability of IN over a limited spatial region. A more comprehensive expression was developed by Phillips et al. (2008), who combined data

ACPD
9, 10957–11004, 2009

from several field campaigns to estimate the contribution of individual aerosol species to the total IN concentration.

Empirical parameterizations are incomplete, as they provide only IN concentrations. Calculation of ice crystal number concentration, N_c, requires the knowledge of cloud supersaturation and therefore the usage of a dynamical framework. Liu and Penner (2005) considered this, and used numerical solutions from a cloud parcel model to correlate N_c to cloud formation conditions (i.e., T, p, V) and the number concentration of individual aerosol species (dust, soot, and sulfate). Although a computationally efficient approach, these correlations are restricted to (largely unconstrained) assumptions regarding the nature of freezing (i.e., the estimation of freezing efficiencies), the size distributions of dust, soot, and sulfate, the mass transfer (i.e., deposition) coefficient of water vapor onto crystals, and, the active freezing mechanisms. Kärcher et al. (2006) proposed a physically based approach to parameterize cirrus cloud formation combining solutions for pure homogeneous (Kärcher and Lohmann, 2002b), and heterogeneous freezing (Kärcher and Lohmann, 2003) into a numerical scheme. Although this approach includes all known relevant factors that determine N_c, it may be computationally intensive; thus, its application is limited to cases where IN can be characterized by a few, well defined, freezing thresholds. Although many cases of atmospheric aerosol can be described this way, it may not be adequate, as even single class aerosol populations usually exhibit a distribution of freezing thresholds (e.g., Meyers et al., 1992; Möhler et al., 2006; Marcolli et al., 2007; Kanji et al., 2008; Phillips et al., 2008; Vali, 2008; Welti et al., 2009). Barahona and Nenes (2009) developed an analytical parameterization that combines homogeneous and heterogeneous freezing within a single expression. Although very fast and with low error (6±33%), this approach is limited to cases where the IN population can be characterized by a single freezing threshold.

This work presents a new physically-based, analytical scheme to parameterize ice cloud formation in a computationally efficient manner. The new scheme addresses all the limitations of previous approaches, allows the usage of both empirical and the-

ACPD
9, 10957–11004, 2009

oretical IN data in a simple dynamical framework, and can consider the full spectral variability in aerosol and IN composition. The new parameterization builds upon the frameworks of Barahona and Nenes (2008, 2009) that combine homogeneous and heterogeneous mechanisms of ice formation, and explicitly resolves the dependency of N_c on conditions of cloud formation (i.e., T, p, V), aerosol number and size, and the freezing characteristics of the IN population.

2 Description of the ice nucleation spectrum

Modeling of ice cloud formation requires a function describing the number concentration of crystals frozen from an aerosol population (i.e., the aerosol freezing fraction) at some temperature, T, and supersaturation, s_i, (known as the "nucleation spectrum"), which is closely related to the nucleation rate coefficient, J, and the freezing probability, P_f. Theoretical studies (e.g., Lin et al., 2002; Khvorostyanov and Curry, 2009) and laboratory experiments (e.g., Tabazadeh et al., 1997a; Koop et al., 2000; Hung et al., 2002; Haag et al., 2003a, b) suggest that J becomes substantially large around some threshold T and s_i (Pruppacher and Klett, 1997). Decreasing T (or increasing s_i) beyond this level exponentially increases J so that (unless s_i is depleted by water vapor deposition onto growing ice crystals) the probability of freezing, P_f, eventually becomes unity (Pruppacher and Klett, 1997; Lin et al., 2002; Khvorostyanov and Curry, 2004; Monier et al., 2006; Barahona and Nenes, 2008). Observations have confirmed this for homogeneous freezing of aqueous droplets, where the threshold s_i and T is confined within a very narrow range of values (Heymsfield and Sabin, 1989; DeMott et al., 1994; Pruppacher and Klett, 1997; Tabazadeh et al., 1997b; Chen et al., 2000; Cziczo and Abbatt, 2001; Khvorostyanov and Curry, 2004) and depends primarily on the water activity within the liquid phase (Koop et al., 2000).

Heterogeneous freezing is different from homogeneous freezing in that it exhibits a broad range of freezing thresholds, even for aerosol of the same type (e.g., Pruppacher and Klett, 1997; Zuberi et al., 2002; Archuleta et al., 2005; Abbatt et al., 2006; Field et

al., 2006; Möhler et al., 2006; Marcolli et al., 2007; Eastwood et al., 2008; Kanji et al., 2008; Khvorostyanov and Curry, 2009). Field campaign data (Meyers et al., 1992; DeMott et al., 1998) and laboratory studies (Field et al., 2006; Möhler et al., 2006; Zobrist et al., 2008; Welti et al., 2009) show that for s_i values larger than the threshold s_i, the aerosol freezing fraction (i.e., P_f) is below unity, increasing with s_i much more slowly than suggested by theory (e.g., Khvorostyanov and Curry, 2005; Phillips et al., 2008; Eidhammer et al., 2009). This discrepancy can be reconciled by assuming that the heterogeneous nucleation rate depends on the local conditions adjacent to individual nucleation sites, rather than on the average characteristics of the aerosol population (i.e., the "singular hypothesis" (e.g., Fletcher, 1969; Vali, 1994)). Freezing occurs instantaneously when threshold s_i and T associated with a nucleation site are reached; thus a distribution of active nucleation sites on the aerosol particles would result in a distribution of freezing thresholds (Marcolli et al., 2007; Zobrist et al., 2007; Vali, 2008; Eidhammer et al., 2009; Khvorostyanov and Curry, 2009). The aerosol freezing fraction is then related to the density of active nucleation sites (which generally depends on the aerosol surface area, particle history, and chemical composition (Pruppacher and Klett, 1997; Abbatt et al., 2006)). Vali (1994, 2008) have argued that $P_f<1$ for each active nucleation site, which may arise if the active sites exhibit transient activity; this implies a temporal dependency of P_f which is however second order on the freezing threshold distribution (Vali, 2008; Khvorostyanov and Curry, 2009).

Experimental studies and field campaign data (e.g., Möhler et al., 2006; Phillips et al., 2008) show that at constant T, the aerosol freezing fraction is well represented by a continuous function of s_i, which results from the diversity of active nucleation sites that may be available in the insoluble aerosol population (Pruppacher and Klett, 1997). If sufficient time is allowed so that transient effects vanish (i.e., P_f is at its maximum), then the "nucleation spectrum" can be defined as,

$$n_s(s_i, T, p, \ldots) = \left.\frac{\partial N_{\text{het}}(s_i, T, p, \ldots)}{\partial s_i}\right|_{T,p,\ldots} \quad (1)$$

where $N_{\text{het}}(s_i, T, p, \ldots)$ is the crystal number concentration produced by heterogeneous

freezing. The subscripts on the right hand side of Eq. (1) indicate that all other state variables (T, p, aerosol concentrations) remain constant when the nucleation spectrum is measured or computed with theory. Therefore, for the remainder of this study, $N_{het}(s_i, T, p, \ldots)$ is represented as $N_{het}(s_i)$ ($n_s(s_i)$ in its differential form), assuming an implicit dependency on other state variables.

2.1 Empirical IN spectra

Developing an ice formation parameterization requires the knowledge of the IN nucleation spectrum in its differential $n_s(s_i)$, or cumulative form, $N_{het}(s_i)$; these can be obtained empirically from field campaign data (Meyers et al., 1992; Phillips et al., 2008), laboratory experiments (e.g., Möhler et al., 2006; Welti et al., 2009) or from nucleation theory (Sect. 2.2).

The simplest form for $n_s(s_i)$ arises by assuming that IN concentrations depend solely on s_i; characteristic examples are the formulations of Meyers et al. (1992, MY92, Table 1) and the background spectrum of Phillips et al. (2007, PDG07, Table 1). MY92 is derived from in-situ measurements of IN concentrations for T between 250 and 266 K and s_i between 2 and 25%. PDG07 is derived from MY92 (after applying an scaling factor to account for the height dependency of IN concentration) and the data of DeMott et al. (2003a). A more comprehensive formulation, considering (in addition to s_i and T) the surface area contribution from different aerosol types (i.e., dust, organic carbon, and soot) and freezing modes (i.e., deposition and immersion), was presented by Phillips et al. (2008, PDA08). PDA08 is developed using IN and aerosol concentration measurements from several field campaigns.

2.2 IN spectra from classical nucleation theory

Theoretical arguments can also be used to obtain an approximate form for the nucleation spectrum. Classical nucleation theory (CNT) suggests that the nucleation rate at two s_i thresholds can be related as (Pruppacher and Klett, 1997; Khvorostyanov and

Curry, 2004)

$$J(s_{i,1}) \approx J(s_{i,2}) \exp\left[-k(T)(s_{i,2} - s_{i,1})\right] \quad (2)$$

where $J(s_{i,1})$ and $J(s_{i,2})$ are the nucleation rate coefficients at $s_{i,1}$ and $s_{i,2}$ respectively; $k(T)$ is a proportionality constant depending on T. Using this, Barahona and Nenes (2008) showed that for pure homogeneous freezing the nucleation spectrum, $N_{\text{hom}}(s_i)$, can be approximated as,

$$N_{\text{hom}}(s_i) \approx N_o \frac{J_{\text{hom}}(s_{\text{hom}})\bar{v}_o}{\alpha V\, k_{\text{hom}}} \frac{1}{(s_{\text{hom}} + 1)} \exp\left[-k_{\text{hom}}(s_{\text{hom}} - s_i)\right] \quad (3)$$

where $J_{\text{hom}}(s_{\text{hom}})$ is the homogenous nucleation rate coefficient at the homogeneous freezing threshold, s_{hom}; N_o and $\bar{v}_o$ are the number concentration and mean volume of the droplet population, respectively, and $k_{\text{hom}}=(s_{\text{hom}}-s_i)^{-1} \ln \frac{J_{\text{hom}}(s_{\text{hom}})}{J_{\text{hom}}(s_i)}$. Equation (3) can be extended to describe heterogeneous nucleation by replacing k_{hom} with a heterogeneous nucleation analog, $k(T)$ (e.g., Pruppacher and Klett, 1997; Khvorostyanov and Curry, 2004, 2009),

$$k(T) = k_{\text{hom}} f_h \quad (4)$$

where $f_h \approx \frac{1}{4}\left(m^3 - 3m + 2\right)$, $m = \cos(\theta)$ and θ is the IN-water contact angle (Fletcher, 1959). Replacing k_{hom} in Eq. (3) with $k(T)$ from Eq. (4), s_{hom} with the heterogeneous freezing threshold, $s_{h,j}$, and, generalizing to an external mixture of *nsp* IN populations, we obtain

$$N_{\text{het}}(s_i) \approx \sum_{j=1,nsp} \min\left\{e_{f,j} N_{a,j} \exp\left[-k_{\text{hom}} f_{h,j}(s_{h,j} - s_i)\right] \;,\; e_{f,j} N_{a,j}\right\} \quad (5)$$

where $s_{h,j}$ is the freezing threshold of the j-th IN population, and, $N_{a,j}$ is the corresponding aerosol number concentration. $e_{f,j} \approx \left[C \frac{J_{h,j}(s_{h,j})\bar{\Omega}_j}{\alpha V\, k(T)} \frac{1}{(s_{h,j}+1)}\right]$ is the freezing efficiency of the j-th population, where $J_{h,j}(s_{h,j})$ is the heterogeneous nucleation rate

ACPD
9, 10957–11004, 2009

coefficient at $s_{h,j}$, and C is a constant that depends on the mean surface area of the j-th aerosol population, $\bar{\Omega}_j$.

The exponential form of Eq. (5) is in agreement with experimental studies (e.g., Möhler et al., 2006). Equation (5) however requires the knowledge of $e_{f,j}$ which in this study is treated as an empirical parameter and used to constrain the maximum freezing fraction of the aerosol population (in reality $e_{f,j}$ is a function of T, aerosol composition and size; these dependencies are analyzed in a companion study). Values for $e_{f,j}$, $s_{h,j}$, and θ_j used in this study (Sect. 4.1, Table 1) are selected from the literature.

3 Formulation of the parameterization

The parameterization is based on the framework of an ascending Lagrangian parcel. At any height during the parcel ascent, supersaturation with respect to ice, s_i, develops and the ice crystal size distribution is determined by heterogeneous freezing of IN, homogeneous freezing of droplets, and growth of existing ice crystals. The solution when homogeneous freezing is the only mechanism active is presented in Barahona and Nenes (2008). The general solution for pure heterogeneous, and, combined homogeneous-heterogeneous freezing is presented in the following sections.

3.1 The ice parcel equations

In the initial stages of cloud formation s_i increases monotonically due to cooling from expansion; growth of crystals, frozen either homogeneously or heterogeneously, increasingly depletes water vapor, up to some level where s_i reaches a maximum, $s_{\max}$ (because water vapor availability balances depletion). At any given point in time, the state of the cloud is determined by the coupled system of equations (Barahona and Nenes, 2009)

$$w_i(t) = \frac{\rho_i}{\rho_a}\frac{\pi}{6}\int \cdots \int_X D_c^3 n_c(D_c, D_{\mathrm{IN}}, m_{1,\ldots,nx}, t) dD_c dD_{\mathrm{IN}} dm_{1,\ldots,nx} \quad (6)$$

ACPD
9, 10957–11004, 2009

$$\frac{ds_i}{dt} = \alpha V(1+s_i) - \beta \frac{dw_i}{dt} \tag{7}$$

$$\frac{dw_i}{dt} = \frac{\rho_i}{\rho_a}\frac{\pi}{2}\int \dots \int_X D_c^2 \frac{dD_c}{dt} n_c(D_c, D_{\mathrm{IN}}, m_{1,\dots,nx}, t) dD_c dD_{\mathrm{IN}} dm_{1,\dots,nx} \tag{8}$$

$$\frac{dD_c}{dt} = \frac{s_i}{\Gamma_1 D_c + \Gamma_2} \tag{9}$$

where $\frac{dw_i}{dt}$ is the rate of water vapor deposition on the ice crystals and V is the updraft velocity. D_c and D_{IN} are the volume-equivalent diameter of the ice crystals and IN, respectively (for homogeneous nucleation D_{IN} is replaced by the size of cloud droplets), $m_{1,\dots,nx}$ collectively represents the mass fractions of the nx chemical species present in the aerosol population (all other symbols are defined in Appendix C). $n_c\left(D_c, D_{l_N}, m_{1,\dots,nx}, t\right)$ is the number distribution of the ice crystals; therefore $n_c(D_c, D_{\mathrm{IN}}, m_{1,\dots,nx}, t) dD_c dD_{\mathrm{IN}} dm_{1,\dots,nx}$ represents the number concentration of ice crystals with sizes in the range $(D_c, D_c + dD_c)$, made from an aerosol particle in the size range $(D_{\mathrm{IN}}, D_{\mathrm{IN}} + dD_{\mathrm{IN}})$, and with composition defined by the interval $(m_{1,\dots,nx}, m_{1,\dots,nx} + dm_{1,\dots,nx})$. X in Eqs. (6) and (8) is the domain of integration and spans over all the values of D_c, D_{IN}, and $m_{1,\dots,nx}$ for which $n_c(D_c, D_{\mathrm{IN}}, m_{1,\dots,nx}, t)$ is defined. The calculation of $w_i(t)$ and $\frac{dw_i}{dt}$ requires the knowledge of $n_c(D_c, D_{\mathrm{IN}}, m_{1,\dots,nx}, t)$, therefore an equation describing the evolution of $n_c(D_c, D_{\mathrm{IN}}, m_{1,\dots,nx}, t)$ should be added to Eqs. (7) to (9). The coupling between n_c, D_c, and s_i in Eqs. (7) to (9) prohibits their analytical solution and are usually numerically integrated (e.g., Lin et al., 2002 and references therein; Kärcher, 2003; Monier et al., 2006; Barahona and Nenes, 2008).

The main parameter of interest resulting from the solution of Eqs. (7) to (9) is the ice crystal number concentration, $N_c = N_{\mathrm{hom}} + N_{\mathrm{het}}$, where N_{hom} and N_{het} are the ice crystal number concentrations from homogeneous and heterogeneous freezing, respectively. N_{hom} can be treated using the analytical approach of Barahona and Nenes (2008), while N_{het} is equal to N_{het} at $s_{\max}$. Therefore, determining N_c requires the computation

of s_{max}. This is accomplished by approximately solving for the root of Eq. (7), which is presented below.

3.2 Determining s_{max} and N_{het}

The size of ice crystals after freezing and growth at any time during the parcel ascent is given by integration of Eq. (9), assuming negligible non-continuum effects on mass transfer (Barahona and Nenes, 2008),

$$D_c(t, s_i) = \left(D_{IN}^2 + \frac{1}{\Gamma_1} \int_{s_o'}^{s_i} \frac{s}{ds/dt} ds \right)^{1/2} \quad (10)$$

where D_{IN} is the initial size of the ice crystals at the moment of freezing and s_o' is the freezing threshold (Barahona and Nenes, 2008). s_o' generally depends on composition and size (Sect. 2), hence, a chemically-heterogeneous, polydisperse IN population can be treated as the superposition of monodisperse, chemically-homogeneous IN classes that differ only in their respective s_o'. This means that Eq. (10) can be applied to each "IN class" of size and composition.

Equation (10) can be simplified assuming that $\frac{1}{\Gamma_1} \int_{s_o'}^{s_i} \frac{s}{ds/dt} ds \gg D_{IN}^2$, which means that the growth experienced by crystals beyond the point of freezing is much larger than their initial size (e.g., Kärcher and Lohmann, 2002b; Nenes and Seinfeld, 2003; Khvorostyanov and Curry, 2005; Monier et al., 2006; Barahona and Nenes, 2009), and is justified given that typical crystal sizes, $D_c > 20\,\mu$m, are much larger than the typical $D_{IN} \sim 1\,\mu$m found in the upper troposphere (e.g., Heymsfield and Platt, 1984; Gayet et al., 2004). Equation (10) is further simplified by considering that the thermodynamic driving force for ice crystal growth (i.e., the difference between s_i and the equilibrium supersaturation) is usually large (s_i generally above 20% (e.g., Lin et al., 2002; Haag

ACPD
9, 10957–11004, 2009

et al., 2003b)). This suggests that crystal growth rates would be limited by water vapor mass transfer rather than by s_i (confirmed by parcel model simulations). Therefore, D_c is a strong function of the crystal residence time in the parcel and weakly dependent on s_i. The limits of the integral in Eq. (10) imply that the crystal residence time is determined by $s_i - s_o^{'}$, therefore Eq. (10) can be rewritten as

$$D_c(t, s_i) \approx D_c(s_i - s_o^{'}) \tag{11}$$

Equations (1) and (11) suggest that Eq. (6) can be written in terms of s_i and $s_o^{'}$,

$$w_i(s_i) = \frac{\pi}{6}\frac{\rho_i}{\rho_a}\int_0^{s_i} D_c^3(s_i - s_o^{'})\, n_s(s_o^{'})\, ds_o^{'} = \frac{\pi}{6}\frac{\rho_i}{\rho_a}\left[D_c^3 \otimes n_s\right](s_i) \tag{12}$$

where $\otimes$ represents the half-convolution product (Appendix A). Taking the derivative of Eq. (12) and substitution into Eq. (7) gives,

$$\frac{ds_i}{dt} = \alpha V(1 + s_i) - \beta\frac{\rho_i}{\rho_a}[g \otimes n_s](s_i) \tag{13}$$

where $g(s_i) = \frac{\pi}{2} D_c^2 \frac{dD_c}{dt}$ is the "growth function" describing the ice crystal volumetric rate of change. Although not explicit in its definition, g, depends on the difference between ambient and equilibrium supersaturation. For a crystal of given $s_o^{'}$, growth proceeds after ambient supersaturation exceeds $s_o^{'}$; therefore, each particle class is characterized by the difference $\Delta s = s_{\max} - s_o^{'}$, and have a unique $g|_{s_{\max}}$ (which depends on T, p, and V), represented as $g(\Delta s)$.

Equation (13) is a simplified supersaturation balance equation used in place of Eq. (7), the root of which (i.e., $\frac{ds_i}{dt} = 0$) gives $s_{\max}$,

$$\alpha V\,(1 + s_{\max}) = \beta\frac{\rho_i}{\rho_a}[g \otimes n_s](s_{\max}) \tag{14}$$

Integrating both sides of Eq. (14) with respect to s_{max} and rearranging we obtain

$$\frac{\alpha V}{\beta \frac{\rho_i}{\rho_a}} \left(s_{max} + \frac{s_{max}^2}{2}\right) = \int_0^{s_{max}} [g \otimes n_s](s)\, ds = \left[\int_0^{s_{max}} g(s)\, ds\right] \left[\int_0^{s_{max}} n_s(s) ds\right] \quad (15)$$

where the identity $\int (f_1 \otimes f_2)(x)dx = \int f_1(u)du \int f_2(v)dv$, (Eq. A5), was employed and allows the partial decoupling of crystal growth and nucleation functions (i.e., the integrals involving g and n_s, respectively) in Eq. (15).

From Eq. (1), $\int_0^{s_{max}} n_s(s)ds = N_{het}(s_{max})$; with this, Eq. (15) can be rewritten as

$$N_{het}(s_{max}) = \frac{\alpha V}{\beta \frac{\rho_i}{\rho_a}} \frac{\left(s_{max} + \frac{s_{max}^2}{2}\right)}{\int_0^{s_{max}} g(\Delta s)\, d(\Delta s)} \quad (16)$$

where the lower and upper limits of the integral in the denominator correspond to the frozen particle with the highest and lowest s_o', respectively. Equation (16) is a general solution of the s_i balance (Eqs. 7 and 13) at s_{max}, and holds regardless of the form of $n_s(s_i)$. $\int_0^{s_{max}} g(\Delta s)\, d(\Delta s)$ still needs to be determined, and depends on the active freezing mechanism present (pure heterogeneous or heterogeneous-homogeneous freezing). $g(\Delta s)$ in general depends on the size of the crystal population at s_{max} and on the form of $n_s(s_i)$ (as crystal nucleation and growth affect the supersaturation profile in the cloud, hence $D_c \frac{dD_c}{dt}$).

3.3 N_{het} under conditions of pure heterogeneous freezing

Equation (16) can be used to calculate N_{het} provided that a suitable expression for $g(\Delta s)$ is available. Assuming that non-continuum effects on mass transfer are negligible

(i.e., the water vapor deposition coefficient, α_d, is equal to unity and D_c is large), then (Appendix B),

$$g_{\alpha_d=1}(\Delta s) \approx \frac{\pi}{2}\frac{s_{\max} D_c(\Delta s)}{\Gamma_1} \tag{17}$$

where Γ_1 is defined in Appendix C, and, $D_c(\Delta s)$ is the size of the crystals at $s_{\max}$ with freezing threshold s_o'. Integrating Eq. (17) from Δs=0 to Δs=$s_{\max}$,

$$\int_0^{s_{\max}} g_{\alpha_d=1}(\Delta s)\, d(\Delta s) = \frac{\pi}{2}\frac{s_{\max}}{\Gamma_1}\int_0^{s_{\max}} D_c(\Delta s)\, d(\Delta s) \tag{18}$$

Direct solution of Eq. (18) is not possible as the functional form of $D_c(\Delta s)$ is in general not known. However, some insight on the form of $\int_0^{s_{\max}} D_c(\Delta s)\, d(\Delta s)$ can be gained by examining the dependency of $D_c(\Delta s)$ on Δs from parcel model simulations. Figure 1 shows $D_c(\Delta s)$ normalized with respect to the maximum size of the crystals at $s_{\max}$ (i.e., those that freeze first in the parcel), $D_{c,\max}$, as a function of $\frac{\Delta s}{s_{\max}}$ for ice cloud formation simulations shown in Tables 1 and 2. Inspection of Fig. 1 suggests that $D_c(\Delta s) \approx D_{c,\max}\left(\frac{\Delta s}{s_{\max}}\right)^{1/n}$, where n is a positive integer which depends on $s_{\max}$. With this we obtain after integration,

$$\int_0^{s_{\max}} D_c(\Delta s)\, d(\Delta s) \approx c(s_{\max}) s_{\max} D_{c,\max} \tag{19}$$

where $c(s_{\max})=\frac{n}{n+1}$ is an integration constant. Substituting Eqs. (17) to (19) into Eq. (16),

$$c(s_{\max}) N_{\text{het}}(s_{\max}) = \frac{\alpha V \Gamma_1}{\beta \frac{\pi}{2}\frac{\rho_i}{\rho_a}} \frac{\left(1+\frac{1}{2}s_{\max}\right)}{s_{\max} D_{c,\max}} \tag{20}$$

$c(s_{max})$ can be constrained so that Eq. (20) reproduces $N_{het}(s_{max})$ at the asymptotic limit of of a monodisperse, chemically-homogeneous IN population for which $N_{het}(s_{max})=N_{het,mono}$. For this, Eq. (7) can be written as (neglecting non-continuum effects on mass transfer),

$$\left.\frac{ds_i}{dt}\right|_{s_{max}} = \alpha V(1+s_{max}) - \beta\frac{\pi}{2}\frac{\rho_i}{\rho_a}N_{het,mono}\frac{s_{max}}{\Gamma_1}D_{c,max} = 0 \quad (21)$$

or

$$N_{het,mono} = \frac{\alpha V\Gamma_1}{\beta\frac{\pi}{2}\frac{\rho_i}{\rho_a}}\frac{(1+s_{max})}{s_{max}D_{c,max}} \quad (22)$$

Equality of N_c between Eqs. (20) and (22) occurs when

$$c(s_{max}) = \frac{1+\frac{1}{2}s_{max}}{1+s_{max}} \quad (23)$$

Equation (23) suggests that as $s_{max}\to\infty$, $c(s_{max})\to\frac{1}{2}$, and, when $s_{max}\to 0$, $c(s_{max})\to 1$ (Fig. 1). It also suggests that the same form for N_{het} applies to the monodisperse and polydisperse expressions of the supersaturation balance (Eqs. 20 and 22), provided that $D_{c,max}$ is the same in both cases. Hence, a characteristic freezing threshold, $s_{h,char}$, for the polydisperse IN population can be defined for which $N_{het,mono}=N_{het}(s_{max})$; $D_{c,max}$ is then a characteristic size of the ice crystal population, $D_{c,char}$ (computed below). The solution for crystal number concentration becomes:

$$N_{het}(s_{max}) = \frac{\alpha V\Gamma_1}{\beta\frac{\pi}{2}\frac{\rho_i}{\rho_a}}\frac{(1+s_{max})}{s_{max}D_{c,char}} \quad (24)$$

Characteristic size of the polydisperse ice crystal population, $D_{c,char}$

A requirement for the equivalence of the polydisperse (Eq. 13) and monodisperse (Eq. 21) expressions of the supersaturation balance is that the rate of water vapor

deposition onto the monodisperse and the polydisperse ice crystal populations at s_{max} is equal, or

$$[D_c \otimes n_s](s_{max}) = N_{het}(s_{max}) D_{c,char} \tag{25}$$

Equation (25) is a Volterra equation of the first kind and can be solved using several analytical and numerical methods (e.g., Linz, 1985). For this, the functional form of $n_s(s_i)$ needs to be known in advance. To keep the parameterization as general as possible, an approximate solution to Eq. (25) is used instead. As N_{het} is a strong function of $D_{c,max}$ (Eqs. 20 and 22), $D_{c,char}$ it is expected to be of the order of $D_{c,max}$. As these crystals grow slowly (owing to their large surface area), their size is to first order a linear function of Δs (Barahona and Nenes, 2009). Therefore, $D_c(\Delta s)$ and $D_{c,char}$ are related by

$$D_c(\Delta s) \approx D_{c,char} \frac{\Delta s}{\Delta s_{char}} \tag{26}$$

where $\Delta s_{char} = s_{max} - s_{h,char}$. Substituting Eq. (26) into Eq. (25), we obtain,

$$[n_s \otimes \Delta s](s_{max}) = N_{het}(s_{max}) \Delta s_{char} \tag{27}$$

which after taking the derivative with respect to s_{max} gives (i.e., Eq. A6),

$$\int_0^{s_{max}} n_s(s) ds = n_s(s_{max}) \Delta s_{char} \tag{28}$$

Application of Eq. (1) to Eq. (28) gives,

$$\Delta s_{char} = \frac{N_{het}(s_{max})}{n_s(s_{max})} \tag{29}$$

If s_{max} is large enough, all IN are frozen and $n_s(s_{max}) \rightarrow 0$; this can lead to numerical instability as Δs_{char} becomes very large. However, a large Δs_{char} also implies that a significant fraction of crystals freeze during the early stages of the parcel ascent so

that, $s_{h,\mathrm{char}} \rightarrow 0$ hence, $\Delta s_{\mathrm{char}} \rightarrow s_{\max}$ and $s_{\max}$ is the upper limit for Δs_{char}. With this, Eq. (29) becomes,

$$\Delta s_{\mathrm{char}} = \min\left(\frac{N_{\mathrm{het}}(s_{\max})}{n_s(s_{\max})}, s_{\max}\right) \tag{30}$$

$D_{c,\mathrm{char}}$ is calculated considering the growth of a monodisperse population with freezing threshold, $s_{h,\mathrm{char}}$ (Barahona and Nenes, 2009),

$$D_{c,\mathrm{char}} = \sqrt{\frac{2\Delta s^*_{\mathrm{char}}}{\alpha V \Gamma_1}} \tag{31}$$

with $\Delta s^*_{\mathrm{char}} = \frac{\Delta s_{\mathrm{char}}\left[\frac{4}{3}\Delta s_{\mathrm{char}} + 2(s_{\max} - \Delta s_{\mathrm{char}})\right]}{(1 + s_{\max} - \Delta s_{\mathrm{char}})}$

Accounting for changes in α_d

If $\alpha_d < 1$, $g(\Delta s)$ should be modified to include the effect of reduced uptake on the growth rate (Barahona and Nenes, 2009). This is done by introducing a correction to $g_{\alpha_d=1}(\Delta s)$ used in Eq. (17),

$$g(\Delta s) \approx f(\alpha_d) g_{\alpha_d=1}(\Delta s) \tag{32}$$

The non-continuum correction factor, $f(\alpha_d)$, is derived in Appendix B; from Eq. (B8),

$$g(s_{\max}) \approx e^{-\frac{2}{\lambda s_{\max}}} g_{\alpha_d=1}(s_{\max}) \tag{33}$$

Equation (33) is substituted into Eqs. (17) to (19) to account for changes in the uptake coefficient or to parameterize processes that limit water vapor mass transfer to growing crystals.

Final form for pure heterogeneous freezing

$N_{het}(s_{max})$ is calculated from combination of Eqs. (24), (31), and (33),

$$\frac{N_{het}(s_{max})}{N^*} = \frac{1}{\sqrt{\Delta s^*_{char}}} \frac{(1+s_{max})}{s_{max}} e^{\frac{2}{\lambda s_{max}}} \tag{34}$$

with $N^* = \sqrt{2}\,(\alpha V \Gamma_1)^{3/2} \left(\beta \frac{\pi}{2} \frac{\rho_i}{\rho_a}\right)^{-1}$. Equation (34) is the solution of the s_i balance (Eq. 14) for pure heterogeneous freezing and shows that $N_{het}(s_{max})$ depends only on s_{max}, N^*, λ, and Δs_{char}. N^* has dimensions of number concentration and represents the ratio of the rate of increase in s_i from expansion cooling to the rate of increase in the surface area of the crystal population. Δs_{char} is related to the steepness of $n_s(s_i)$ about s_{max}; a value of $\Delta s_{char} \rightarrow 0$ implies that most of the crystals freeze at s_i close to s_{max}. λ accounts for non-continuum effects; if the crystal concentration is low ($\sim$ less than 0.01 cm^{-3}) and $\Delta s_{char} \rightarrow s_{max}$ then size effects on $N_{het}(s_{max})$ can usually be neglected. Equation (34) is solved along with an expression for $N_{het}(s_{max})$ to find s_{max} (Sect. 3.5, Fig. 2).

3.4 Competition between homogeneous and heterogeneous freezing

At T below 235 K, ice clouds form primarily from homogeneous freezing (e.g., Heymsfield and Sabin, 1989; DeMott et al., 2003a; Barahona and Nenes, 2009). If a significant concentration of IN is present, freezing of IN prior to the onset of homogeneous nucleation may inhibit droplet freezing (Gierens, 2003; Barahona and Nenes, 2009). Equations (7) to (9) can be readily extended to account for this, for which a generalized nucleation spectrum is defined that includes contribution from homogeneous freezing of droplets. This is simplified if taken into account that homogeneous nucleation rates are very high, and, the nucleation spectrum is close to being a delta function about $s_i = s_{hom}$. Furthermore, since the number concentration of liquid droplets available for

ACPD
9, 10957–11004, 2009

freezing is much greater than the concentration of IN (i.e., $N_o \gg N_{het}$), s_{max} is reached soon after homogeneous freezing is triggered ($s_{max} \approx s_{hom}$) (Kärcher and Lohmann, 2002a; Barahona and Nenes, 2008). IN freezing thresholds are generally lower than s_{hom}; homogeneous freezing can always be considered the last freezing step during ice cloud formation.

As the growth of previously frozen crystals reduces the rate of increase of s_i, (i.e., $\left.\frac{ds_i}{dt}\right|_{s_{hom}}$), the presence of IN tends to reduce homogeneous freezing probability and the ice crystal concentration (compared to a pure homogeneous freezing event). The droplet freezing fraction, f_c, in the presence of IN is proportional to the decrease in $\left.\frac{ds_i}{dt}\right|_{s_{hom}}$ (Barahona and Nenes, 2009) from the presence of IN, i.e.,

$$f_c = f_{c,hom} \left(\frac{\left.\frac{ds_i}{dt}\right|_{s_{hom}}}{\alpha V (s_{hom} + 1)} \right)^{3/2} \tag{35}$$

where $\alpha V(s_{hom}+1)$ is an approximation to $\left.\frac{ds_i}{dt}\right|_{s_{hom}}$ when IN are not present, and, $f_{c,hom}$ is the droplet freezing fraction under pure homogeneous conditions, given by Barahona and Nenes (2008). Although Eq. (35) is derived for a monodisperse IN population, Eqs. (16) and (23) suggest that the effect of the polydisperse IN population can be expressed as a monodisperse population, provided that a suitable characteristic freezing threshold, $s_{h,char}$, is defined. Extending the monodisperse IN population solution (Barahona and Nenes, 2009) to a polydisperse aerosol gives,

$$\frac{\left.\frac{ds_i}{dt}\right|_{s_{hom}}}{\alpha V (s_{hom} + 1)} \approx 1 - \left(\frac{N_{het}(s_{hom})}{N_{lim}} \right)^{3/2} \tag{36}$$

where $N_{het}(s_{hom})$ is calculated from the nucleation spectrum function (Sect. 2), and N_{lim} is the limiting IN concentration that completely inhibits homogeneous freezing (Bara-

ACPD
9, 10957–11004, 2009

hona and Nenes, 2009). If $N_{het}(s_{hom})$ is such that $s_{max}=s_{hom}$, then all IN concentrations greater than $N_{het}(s_{hom})$ would result in a $s_{max}<s_{hom}$ and prevent homogeneous freezing (i.e., heterogeneous freezing would be the only mechanism forming crystals). Conversely, if the IN concentration is lower than $N_{het}(s_{hom})$ and $s_{max}>s_{hom}$, homogeneous freezing is active. Thus, N_{lim} must be equal to $N_{het}(s_{hom})$ at $s_{max}=s_{hom}$, and is obtained by substituting $s_{max}=s_{hom}$ into Eq. (34), i.e.,

$$\frac{N_{lim}}{N^*} = \frac{1}{\sqrt{\Delta s^*_{char}\big|_{s_{hom}}}} \frac{(1+s_{hom})}{s_{hom}} e^{\frac{2}{\lambda s_{hom}}} \tag{37}$$

For very low N_{het}, Eq. (35) approaches the pure homogeneous freezing limit as the effect of IN is negligible; homogeneous freezing is prevented for $N_{het}(s_{hom}) \geq N_{lim}$ and $f_c \leq 0$. Thus, combination of Eqs. (34) and (35) provides the total crystal concentration, N_c, from the combined effects of homogeneous and heterogeneous freezing (Barahona and Nenes, 2009),

$$N_c = \begin{cases} N_o e^{-f_c}(1-e^{-f_c}) + N_{het}(s_{hom}) & f_c>0 \text{ and } T<235\,\text{K} \\ N_{het}(s_{max}) & f_c \leq 0 \text{ or } T>235\,\text{K} \end{cases} \tag{38}$$

Equation (38) accounts for the fact that homogeneous freezing is not probable for $T>235$ K (e.g., Pruppacher and Klett, 1997).

3.5 Implementation of the parameterization

The generalized parameterization presented in this study is fairly simple to apply and outlined in Fig. 2. Inputs to the parameterization are cloud formation conditions (i.e., p, T, V), liquid droplet and IN aerosol number concentration (i.e, N_o, N_{dust}, N_{soot}). Additional inputs (i.e., $s_{h,j}, \theta_j$) may be required depending on the expression used for the nucleation spectrum, $N_{het}(s_i)$. If $T<235$ K, the procedure starts by calculating $N_{het}(s_{hom})$, N_{lim} (Eq. 37) and then f_c (Eqs. 35 and 36). If $f_c>0$, then N_c is given by the application of Eq. (38) with $f_{c,hom}$ from Barahona and Nenes (2008). If $f_c \leq 0$ or

ACPD
9, 10957–11004, 2009

$T>235$ K, heterogeneous freezing is the only mechanism active, and $N_c=N_{het}(s_{max})$, obtained by numerically solving Eq. (34). Alternatively, precalculated lookup tables or approximate explicit solutions to Eq. (34) can be used to avoid iterative solutions.

4 Evaluation and discussion

The parameterization is tested for all the nucleation spectra presented in Table 1. Only dust and black carbon species are considered, as the contribution of organic carbon to the IN population is about six times lower than that of black carbon (Phillips et al., 2008). The total surface area of each aerosol population is scaled using the base size distributions of Phillips et al. (2008). A simple linear relation is employed to diagnose $e_{f,j}$, being about 0.05 for dust and soot aerosol particles at $s_i=s_h$ (Pruppacher and Klett, 1997) and decreasing linearly for $s_i<s_h$ (Table 1). Freezing thresholds were set to $s_{h,dust}=0.2$ (Kanji et al., 2008) and $s_{h,soot}=0.3$ (Möhler et al., 2005); θ_{dust} was set to 16° ($m_{dust}=0.96$) and θ_{soot} to 40° ($m_{soot}=0.76$)(Chen et al., 2008). k_{hom} is calculated based on Koop et al. (2000) using the fitting of Barahona and Nenes (2008, 2009); s_{hom} is obtained from the analytical fit of Ren and Mackenzie (2005).

4.1 Comparison against parcel model results

The parameterization was compared against the numerical solution of Eqs. (7) to (9) using the model of Barahona and Nenes (2008, 2009), for all nucleation spectra of Table 1, and conditions of Table 2 (about 1200 simulations overall). To independently test the accuracy of Eqs. (34) and (38), simulations were made under conditions of pure heterogeneous and combined homogeneous-heterogeneous freezing. Calculated N_c ranged from 10^{-4} to 10^2 cm^{-3}; s_{max} ranged (in absolute units) from 0.05 to 1 for pure heterogeneous freezing and from 0.05 to 0.6 for combined homogeneous-heterogeneous freezing, which covers the expected range of conditions encountered in a GCM simulation.

ACPD
9, 10957–11004, 2009

Figure 3 shows s_{max} (calculated solving Eq. (34)) vs. the parcel model results for conditions of pure heterogeneous freezing. The statistical analysis of the comparison is shown in Table 3 for all nucleation spectra of Table 1 and conditions of Table 2. The overall error with respect to parcel model results is −1.68±3.42%, which is remarkably low, given the complexity of Eqs. (7) to (9), and the diversity of $N_{het}(s_i)$ expressions used (Table 1). Among the nucleation spectra tested, the largest variability was obtained when using the PDA08 (−2.69±2.81%) and CNT (−1.56±4.14%) spectra. This results from variations in the form of the $N_{het}(s_i)$ function; the distribution functions, $n_s(s_i)$, for MY92 and PDG07 are monotonically increasing and smooth (e.g., Fig. 6) over the entire s_i range considered. PDA08 and CNT are characterized by abrupt changes in $N_{het}(s_i)$ which produces discontinuities in $n_s(s_i)$. This is evident for the CNT spectrum as the error in the calculation of s_{max} lowers (−1.7±2.5%) if only data with $s_{max}<s_{h,soot}$ is considered. CNT also shows an slight overestimation of s_{max} at high values caused by the assumption of $s_{h,char}=0$ when $n_s(s_i)=0$, Eq. (30); this however is not a source of uncertainty for N_{het} calculation (Fig. 4) as crystal concentration is constant for $s_{max}>s_{h,soot}$ (Table 1). Another source of discrepancy is the small change in T (∼4 K), from $s_i=0$ to $s_i=s_{max}$ which is larger at high V and causes an slight underestimation of s_{max} at high values (∼$s_{max}>0.7$) for the PDG07 and MY92 spectra, which is however never outside of the ±5% range.

Figure 4 shows that the error in N_{het} calculation is also quite low, −2.0±8.5%, which indicates no biases in the parameterization. The slightly larger error in N_c compared to the error in s_{max} originates from the sensitivity of $N_{het}(s_{max})$ to small variations in s_{max}. Figure 6 shows that the larger discrepancy in s_{max} when using the CNT and PDA08 spectra does not translate into a large error in N_{het} which remains low for these cases (∼5%). The largest variability (±13.5%) was found using MY92 and is related to the slight underestimation of s_{max} at high V ($s_{max}>0.7$). Δs_{char} for MY92 is around 0.07 (whereas for the other spectra of Table 1 it is generally above 0.2) which indicates that most crystals in the MY92 spectrum freeze at s_i close to s_{max} (Eq. 30); therefore MY92 is most sensitive to the small underestimation in s_{max} at high V.

When competition between homogeneous and heterogeneous nucleation is considered (Fig. 5), $s_{max} \approx s_{hom}$, and no explicit dependency of N_c on s_{max} is considered; this approximation however does not introduce substantial error in the calculation of N_c (Barahona and Nenes, 2008). The overall error in N_c calculation for this case is 4.7±21%. Comparison of Figs. 4 and 5 suggest that most of the error results from the inherent error of the homogeneous nucleation scheme (1±28%, (Barahona and Nenes, 2008)). Figure 5 shows that the parameterization reproduces the parcel model results from the pure heterogeneous (i.e., $\frac{N_{het}}{N_{lim}} > 1$) to the pure homogeneous (i.e., $\frac{N_{het}}{N_{lim}} \rightarrow 0$) freezing limit. The largest discrepancy (−9.6±21%) occurs when the PDA08 spectrum is used, and is related to the complexity of the $N_{het}(s_i)$ function. Larger variations (mostly within a factor of 2) also occur when $N_{het}(s_{max}) \rightarrow N_{lim}$ and are caused by the high sensitivity of N_c to $N_{het}(s_{max})$ for $\frac{N_{het}}{N_{lim}} \approx 1$ (cf., Barahona and Nenes, 2009, Fig. 3).

4.2 Comparison against existing schemes

The new parameterization was compared against the schemes of Liu and Penner (2005, LP05) and Kärcher et al. (2006, K06), for all spectra of Table 1 and, for T=206 K, p=22000 Pa, and, α_d=0.5. Consistent with K06, the maximum number concentration of IN was set to 0.005 cm^{-3}, which for $e_{f,soot}$=0.05 implies N_{soot}=0.1 cm^{-3}. Cases with no dust present (i.e., N_{dust}=0 and no deposition freezing in LP05) and with $N_{dust}=N_{soot}$ were considered. For the "no-dust" case (Fig. 6, left) K06 and the new parameterization (Eq. 38, using the CNT, MY92, and PDG07 spectra), agree within a factor of two at the pure heterogeneous limit ($\sim V < 0.01$ m s^{-1}). Homogenous freezing in these cases is triggered (i.e., $N_{lim} > N_{het}$) between 0.03 and 0.07 m s^{-1} except when using MY92 where $V > 0.7$ m s^{-1} is needed to allow homogeneous freezing. When using Eq. (38) and PDA08, a much lower N_{het} is predicted over the entire V range considered, and homogeneous freezing is triggered at very low $V \sim 0.002$ m s^{-1} (i.e., heterogeneous freezing has a negligible effect on N_c). LP05 predicts N_{het} about two orders of magnitude larger than the application of Eq. (38) to the PDG07 and CNT

ACPD
9, 10957–11004, 2009

spectra. This discrepancy may result from the high $e_{f,\mathrm{soot}}$~1 (which is evident for V>0.04 m s^{-1}as N_{het}≈N_{soot}) implied in this parameterization compared to the other freezing spectra considered. LP05 predicts complete inhibition of homogeneous freezing up to V~0.3 m s^{-1} which is much larger than the range between 0.03 and 0.07 m s^{-1} found by application of Eq. (38).

When similar concentrations of dust and soot are considered (Fig. 6 right), Eq. (38) with PDA08 come much closer to simulations using CNT and PDG07. K06 (maintaining N_{IN}=0.005 cm^{-3}) still lies within a factor of two from the results obtained with Eq. (38) and the CNT, PDA08, and PDG07 spectra. By including dust, the onset of homogeneous nucleation is triggered at slightly higher V, compared to the case with no dust (CNT). For PDA08 the change is more pronounced, indicating that the maximum $e_{f,\mathrm{dust}}$ implied by PDA08 is substantially larger than $e_{f,\mathrm{soot}}$ for the same spectrum, i.e., most of the crystals in this case come from freezing of dust. At the pure homogeneous freezing limit (V~1 m s^{-1}), IN effects on N_c are unimportant, and, N_c for all spectra agree well with K06 (Barahona and Nenes, 2008). At this limit, LP05 predicts a twofold higher N_c due to the lower value of α_d=0.1 used in developing LP05 compared to α_d=0.5 used in generating Fig. 6.

A comparison of predicted s_{max} between the new parameterization and LP05 was also carried out. The curves of Fig. 7 can be used to explain the profiles of Fig. 6, as homogeneous freezing is prevented if s_{max}<s_{hom} (Gierens, 2003; Barahona and Nenes, 2009). When dust is not included, s_{max} calculated using PDA08 approaches s_{hom} at very low V, therefore allowing homogeneous nucleation to take place in almost the entire range of V considered. When dust is included, s_{max} calculated using Eq. (38) and the PDG07, PDA08 and CNT spectra approaches s_{hom} for V between 0.02 and 0.06 m s^{-1}. When using MY92, s_{max} is below s_{hom} for almost the entire range of V considered, and, explains why homogeneous freezing is prevented for most values of V. LP05 predicts a very different s_{max} profile , being constant (s_{max}~0.2) at low V, then a steep increase in s_{max} around V~0.1 m s^{-1} which reaches s_{hom} at V~0.3 m s^{-1}.

5 Summary and conclusions

We present an ice cloud formation parameterization that calculates N_c and s_{max} explicitly considering the competition between homogeneous and heterogeneous freezing from a polydisperse (in size and composition) aerosol population. Heterogeneous freezing is accounted for by using a nucleation spectrum that could have any functional form. Analytical solution of the parcel model equations was accomplished by reformulating the supersaturation balance and by introducing the concepts of characteristic freezing threshold and characteristic size of a polydisperse ice crystal population. The approach presented here successfully decouples the nucleation and growth factors in the solution of the supersaturation balance, and together with the work of Barahona and Nenes (2008, 2009), provides a comprehensive parameterization for ice cloud formation. The parameterization was tested with a diverse set of published IN spectra (Table 1), which includes a formulation introduced here derived from classical nucleation theory.

When evaluated over a wide set of conditions and IN nucleation spectra the parameterization reproduced detailed numerical parcel model results to −1.6±3.4% and −2.0±8.5%, for the calculation of s_{max} and N_{het} from pure heterogeneous freezing, respectively, and 4.7±21% for the calculation of N_c from combined homogeneous and heterogeneous freezing. Comparison against other formulations over a limited set of conditions showed that the freezing efficiency of the different IN populations (i.e., dust and soot) is the main factor determining the effect of heterogeneous freezing on the total ice crystal concentration, N_c. The variability of N_c shown in Fig. 6 is however much lower than reported by Phillips et al. (2008), who compared several nucleation spectra at fixed s_i; this emphasizes the importance of using a proper dynamic framework in comparing nucleation spectra.

The parameterization presented in this work is computationally efficient and analytically unravels the dependency of ice crystal concentration on cloud formation conditions (T, p, V), deposition coefficient, the size and composition of the droplet popula-

ACPD
9, 10957–11004, 2009

tion, and insoluble aerosol (i.e., IN) concentrations. It comprehensively addresses all the shortcomings of previous approaches and provides a framework in which new ice nucleation data can easily be understood and incorporated into global climate studies.

Appendix A

The convolution product

Let f_1 and f_2 be two locally integrable functions over the real axis, then the function

$$(f_1 * f_2)(x) = \int_0^\infty f_1(v) f_2(x - v) dv \tag{A1}$$

is called the convolution product of the functions f_1 and f_2 (Kecs, 1982). The half-convolution product (or convolution of the half-axis) is defined for $x \geq 0$ as

$$(f_1 \otimes f_2)(x) = \int_0^x f_1(v) f_2(x - v) dv \tag{A2}$$

and related to the convolution product by

$$(f_1 \otimes f_2)(x) = [\mathrm{H}(f_1) * \mathrm{H}(f_2)](x) \tag{A3}$$

where H is the Heaviside function,

$$\mathrm{H}(v) = \begin{cases} 0, & v < 0 \\ 1, & v \geq 0 \end{cases} \tag{A4}$$

The convolution product is commutative and distributive; its integral is given by

$$\int (f_1 * f_2)\, dx = \int f_1(u) du \int f_2(v) dv \tag{A5}$$

ACPD
9, 10957–11004, 2009

its derivative is expressed as

$$\frac{d}{dx}(f_1 * f_2)(x) = \left(\frac{df_1}{dx} * f_2\right)(x) = \left(f_1 * \frac{df_2}{dx}\right)(x) \quad \text{(A6)}$$

Appendix B

Analytical correction for non-continuum effects

The growth expression of a monodiperse ice crystal population (Barahona and Nenes, 2008, 2009) can be used to approximate the size of an ice crystal that freezes at supersaturation s_o' during the parcel ascent,

$$D_c(\Delta s) = -\frac{\Gamma_2}{\Gamma_1} + \sqrt{\left(\frac{\Gamma_2}{\Gamma_1}\right)^2 + \frac{\Delta s^2}{\alpha V \Gamma_1}} \quad \text{(B1)}$$

which can be written as

$$D_c(\Delta s) = \gamma\left[\sqrt{1 + (\lambda \Delta s)^2} - 1\right] \quad \text{(B2)}$$

where $\gamma = \frac{\Gamma_2}{\Gamma_1}$, $\lambda = \sqrt{\frac{1}{\alpha V \Gamma_1 \gamma^2}}$. After substituting Eq. (B2) into Eq. (9) and rearranging, the growth function at $s_{\max}$, $g(\Delta s) = \frac{\pi}{2} D_c^2 \frac{dD_c}{dt} = \frac{\pi}{2} \frac{s_{\max} D_c^2}{\Gamma_1 D_c + \Gamma_2}$, can be written in the form

$$g(\Delta s) = \frac{\pi}{2} \frac{s_{\max}}{\Gamma_1} \frac{\gamma\left(1 - \sqrt{1 + (\lambda \Delta s)^2}\right)^2}{\sqrt{1 + (\lambda \Delta s)^2}} \quad \text{(B3)}$$

If non-continuum effects on mass transfer are neglected, then, $\Gamma_1 \gg \Gamma_2$ and Eq. (B1) becomes

$$D_c(\Delta s) = \gamma \lambda \Delta s \quad \text{(B4)}$$

ACPD
9, 10957–11004, 2009

Equation (B4) is mostly applicable when α_d=1; the growth function for this case is represented as $g_{\alpha_d=1}$, and given by

$$g_{\alpha_d=1}(\Delta s) = \frac{\pi}{2}\frac{s_{\max}}{\Gamma_1}\gamma\lambda\Delta s \tag{B5}$$

for values of α_d below unity, Eqs. (B2) and (B3) should be applied to calculate $g(\Delta s)$. An approximate relation between $g(\Delta s)$ and $g_{\alpha_d=1}(\Delta s)$ can be found by dividing Eq. (B5) by Eq. (B3),

$$\frac{g_{\alpha_d=1}}{g} = \frac{\lambda\Delta s\sqrt{1+(\lambda\Delta s)^2}}{\left(1-\sqrt{1+(\lambda\Delta s)^2}\right)^2} \tag{B6}$$

Equation (B6) shows that $\frac{g_{\alpha_d=1}}{g}$ is determined by the product $\lambda\Delta s$; Eq. (19) suggests that $\lambda s_{\max}$ is a characteristic value for $\lambda\Delta s$, so that Eq. (B6) can rewritten as

$$\frac{g_{\alpha_d=1}}{g} \approx \frac{\lambda s_{\max}\sqrt{1+\lambda^2 s_{\max}^2}}{\left(1-\sqrt{1+\lambda^2 s_{\max}^2}\right)^2} \tag{B7}$$

For $s_{\max}$>0.05, Eq. (B7) can be approximated by

$$\frac{g_{\alpha_d=1}}{g} \approx e^{2/\lambda s_{\max}} \tag{B8}$$

ACPD
9, 10957–11004, 2009

Appendix C

List of symbols and abbreviations

α	$\frac{g\Delta H_s M_w}{c_p RT^2} - \frac{a_g M_a}{RT}$
α_d	Water vapor to ice deposition coefficient
a_g	Acceleration of gravity
β	$\frac{M_a p}{M_w p_i^o} - \frac{\Delta H_s^2 M_w}{c_p RT^2}$
γ	$\frac{\Gamma_2}{\Gamma_1}$
$c(s_{\max})$	Integration constant defined in Eq. (23)
c_p	Specific heat capacity of air
$D_{c,\mathrm{char}}$	Characteristic size of the ice crystal population
D_c	Volume sphere-equivalent diameter of an ice particle
$D_{c,\max}$	Size of the largest crystals at $s_{\max}$
ΔH_s	Enthalpy of sublimation of water
D_{IN}	Volume sphere-equivalent diameter of an IN
Δs	$s_{\max} - s_o^{'}$
$\Delta s^*_{\mathrm{char}}$	Growth integral, defined by Eq. (31)
D_v	Water vapor mass transfer coefficient
$e_{f,j}$	Maximum freezing efficiency of the j-th IN species
$f_{c,\mathrm{hom}}$, f_c	Fraction of frozen particles at s_{hom} with and without IN present, respectively.

ACPD
9, 10957–11004, 2009

Continued.

$f_{h,j}$	Shape factor of the j-th IN species
$g(\Delta s),\ g(s_i)$	Ice crystal population growth function, $\frac{\pi}{2} D_c^2 \frac{dD_c}{dt}$
$g(\Delta s)_{\alpha_d=1}$	Growth function for $\alpha_d = 1$
Γ_1	$\frac{\rho_i RT}{4 p_i^o D_v M_w} + \frac{\Delta H_s \rho_i}{4 k_a T} \left(\frac{\Delta H_s M_w}{RT} - 1 \right)$
Γ_2	$\frac{\rho_i RT}{2 p_i^o M_w} \sqrt{\frac{2\pi M_w}{RT}} \frac{1}{\alpha_d}$
H	Heaviside's function
$J(s_i),\quad J$	Nucleation rate coefficient at s_i
$J_{\text{hom}}(s_{\text{hom}})$	Homogenous nucleation rate coefficient at s_{hom}
$J_{h,j}(s_{h,j})$	Heterogeneous nucleation rate coefficient at the freezing threshold of the j-th IN population
$k(T)$	Freezing parameter defined by Eq. (2)
k_a	Thermal conductivity of air
k_{hom}	Homogeneous freezing parameter, $\ln \frac{J_{\text{hom}}(s_{\text{hom}})}{J_{\text{hom}}(s_i)} (s_{\text{hom}} - s_i)^{-1}$
λ	$\sqrt{\frac{1}{\alpha V \Gamma_1 \gamma^2}}$
$m_{1\ldots nx}$	Multidimensional variable that symbolizes the mass fraction of the nx chemical species present in an aerosol population

ACPD
9, 10957–11004, 2009

Continued.

m_j	Wettability parameter of the j-th IN species, $\cos(\theta_j)$
M_w, M_a	Molar masses of water and air, respectively
N^*	$\sqrt{2}\,(\alpha V\,\Gamma_1)^{3/2}\left(\beta\frac{\pi}{2}\frac{\rho_i}{\rho_a}\right)^{-1}$
$N_{a,j}$	Number concentration of the j-th insoluble aerosol species
N_c	Total ice crystal number concentration
$n_c(D_c, D_{IN}, m_{I\ldots nx}, t)$	Number distribution of the ice crystals
N_{dust}	Dust number concentration
N_{soot}	Soot number concentration
$N_{\text{het,mono}}$	Monodisperse ice crystal number concentration from heterogeneous freezing
N_{het}	Ice crystals number concentration from heterogeneous freezing
$N_{\text{het}}(s_i)$	Cumulative heterogeneous nucleation spectrum
$N_{\text{hom}}(s_i)$	Cumulative homogeneous nucleation spectrum
N_{IN}	Maximum IN number concentration
N_{lim}	Limiting N_{IN} that would prevent homogeneous nucleation
N_o	Number concentration of the supercooled liquid droplet population
$n_s(s_i)$	Heterogeneous nucleation spectrum
nsp	Number of externally mixed IN populations
nx	Number of chemical species present in the aerosol population

ACPD
9, 10957–11004, 2009

Continued.

p	Ambient pressure
P_f	Freezing probability
p_i^o	Ice saturation vapor pressure
R	Universal gas constant
ρ_i, ρ_a	Ice and air densities, respectively
$s_{h,j}$	Freezing threshold of the *jth* IN species
$s_{h,\text{char}}$	Characteristic freezing threshold of the heterogeneous IN population
s_{hom}	Homogeneous freezing threshold
s_i	Water vapor supersaturation ratio with respect to ice
s_{max}	Maximum ice supersaturation ratio
$s_o^{'}$	Freezing threshold of an IN
T	Temperature
T_o	Initial temperature of the cloudy parcel
t	Time
θ_j	Contact angle between the j^{th} IN species surface and water
V	Updraft velocity
$\bar{v}_o$	Mean volume of the droplet population
w_i	Ice mass mixing ratio
X	Domain of integration in Eq. (6)
$\bar{\Omega}_j$	Mean surface area of the j-th insoluble aerosol population

ACPD
9, 10957–11004, 2009

Acknowledgements. This study was supported by NASA MAP, NASA ACMAP and a NASA New Investigator Award.

References

Abbatt, J. P. D., Benz, S., Cziczo, D. J., Kanji, Z., and Möhler, O.: Solid ammonium sulfate as ice nuclei: a pathway for cirrus cloud formation, Science, 313, 1770–1773, 2006.

Archuleta, C. M., DeMott, P. J., and Kreidenweis, S. M.: Ice nucleation by surrogates for atmospheric mineral dust and mineral dust/sulfate particles at cirrus temperatures, Atmos. Chem. Phys., 5, 2617–2634, 2005, http://www.atmos-chem-phys.net/5/2617/2005/.

Baker, M. B. and Peter, T.: Small-scale cloud processes and climate, Nature, 451, 299–300, 2008.

Barahona, D. and Nenes, A.: Parameterization of cirrus formation in large scale models: Homogenous nucleation, J. Geophys. Res., 113, D11211, doi:11210.11029/12007JD009355, 2008.

Barahona, D. and Nenes, A.: Parameterizing the competition between homogeneous and heterogeneous freezing in cirrus cloud formation monodisperse ice nuclei, Atmos. Chem. Phys., 9, 369–381, 2009, http://www.atmos-chem-phys.net/9/369/2009/.

Chen, J.-P., Hazra, A., and Levin, Z.: Parameterizing ice nucleation rates using contact angle and activation energy derived from laboratory data, Atmos. Chem. Phys., 8, 7431–7449, 2008, http://www.atmos-chem-phys.net/8/7431/2008/.

Chen, Y., DeMott, P. J., Kreidenweis, S. M., Rogers, D. C., and Sherman, D. E.: Ice formation by sulfate and sulfuric acid aerosol particles under upper-tropospheric conditions, J. Atmos. Sci., 57, 3752–3766, 2000.

Cziczo, D. J. and Abbatt, J. P. D.: Ice nucleation in NH_4HSO_4, NH_4NO_3, and H_2SO_4 aqueous particles: Implications for cirrus formation, Geophys. Res. Lett., 28, 963–966, 2001.

DeMott, P. J., Meyers, M. P., and Cotton, R. W.: Parameterization and impact of ice initiation processes relevant to numerical model simulations of cirrus clouds, J. Atmos. Sci., 51, 77–90, 1994.

DeMott, P. J., Rogers, D. C., and Kreidenweis, S. M.: The susceptibility of ice formation in upper tropospheric clouds to insoluble aerosol components, J. Geophys. Res., 102, 19575–19584, 1997.

DeMott, P. J., Rogers, D. C., Kreidenweis, S. M., Chen, Y., Twohy, C. H., Baumgardner, D. G., Heymsfield, A. J., and Chan, K. R.: The role of heterogeneous freezing nucleation in upper tropospheric clouds: Inferences from SUCCESS, Geophys. Res. Lett., 25, 1387–1390, 1998.

DeMott, P. J., Cziczo, D. J., Prenni, A. J., Murphy, D. M., Kreidenweis, S. M., Thompson, D. S., Borys, R., and Rogers, D. C.: Measurements of the concentration and composition of nuclei for cirrus formation, Proc. Natl. Acad. Sci. USA, 100, 14655–14660, 2003a.

DeMott, P. J., Sassen, K., Poellot, M. R., Baumgardner, D. G., Rogers, D. C., Brooks, S. D., Prenni, A. J., and Kreidenweis, S. M.: African dust aerosols as atmospheric ice nuclei, Geophys. Res. Lett., 30, 1732, doi:1710.1029/2003GL017410, 2003b.

Eastwood, M. L., Cremel, S., Gehrke, C., Girard, E., and Bertram, A. K.: Ice nucleation on mineral dust particles: Onset conditions, nucleation rates and contact angles, J. Geophys. Res., 113, D22203, doi:22210.21029/22008JD10639, 2008.

Eidhammer, T., DeMott, P. J., and Kreidenweis, S. M.: A comparison of heterogeneous ice nucleation parameterizations using a parcel model framework, J. Geophys. Res., 114, doi:10.1029/2008JD011095, 2009.

Field, P. R., Möhler, O., Connolly, P., Krämer, M., Cotton, R., Heymsfield, A. J., Saathoff, H., and Schnaiter, M.: Some ice nucleation characteristics of Asian and Saharan desert dust, Atmos. Chem. Phys., 6, 2991–3006, 2006, http://www.atmos-chem-phys.net/6/2991/2006/.

Fletcher, H. N.: On ice-crystal production by aerosol particles, J. Atmos. Sci., 16, 173–180, 1959.

Fletcher, H. N.: Active sites and ice crystal nucleation, J. Atmos. Sci., 26, 1266–1271, 1969.

Gayet, J. F., Ovarlez, J., Shcherbakov, V., Ström, J., Schumann, U., Minikin, A., Auriol, F., Petzold, A., and Monier, M.: Cirrus cloud microphysical and optical properties at southern and northern midlatitudes during the INCA experiment, J. Geophys. Res., 109, D20206, doi:20210.21029/22004JD004803, 2004.

Gierens, K.: On the transition between heterogeneous and homogeneous freezing, Atmos. Chem. Phys., 3, 437–446, 2003, http://www.atmos-chem-phys.net/3/437/2003/.

Haag, W., Kärcher, B., Schaefers, S., Stetzer, O., Möhler, O., Schurath, U., Krämer, M., and Schiller, C.: Numerical simulations of homogeneous freezing processes in the aerosol chamber AIDA, Atmos. Chem. Phys., 3, 195–210, 2003a, http://www.atmos-chem-phys.net/3/195/2003/.

Haag, W., Kärcher, B., Strom, J., Minikin, A., Lohmann, U., Ovarlez, J., and Stohl, A.: Freezing

thresholds and cirrus formation mechanisms inferred from in situ measurements of relative humidity, Atmos. Chem. Phys., 3, 1791–1806, 2003b, http://www.atmos-chem-phys.net/3/1791/2003/.
Hartmann, D. L., Holton, J. R., and Fu, Q.: The heat balance of the tropical tropopause, cirrus, and stratospheric dehydration, Geophys. Res. Lett., 28, 1969–1972, 2001.
Heymsfield, A. J. and Platt, C. M.: A parameterization of the particle size spectrum of ice clouds in terms of the ambient temperature and ice water content, J. Atmos. Sci., 41, 846–855, 1984.
Heymsfield, A. J., and Sabin, R. M.: Cirrus crystal nucleation by homogenous freezing of solution droplets., J. Atmos. Sci., 46, 2252–2264, 1989.
Hung, H., Malinowski, A., and Martin, S. T.: Ice nucleation kinetics of aerosols containing aqueous and solid ammonium sulfate, J. Phys. Chem. A, 106, 293–306, 2002.
Kanji, Z. A., Florea, O., and Abbatt, J. P. D.: ice formation via deposition nucleation on mineral dust and organics: dependence of onset relative humidity on total particulate surface area, Environ. Res. Lett., 3, doi:10.1088/1748-9326/1083/1082/025004, 2008.
Kärcher, B. and Lohmann, U.: A parameterization of cirrus cloud formation: homogeneous freezing of supercooled aerosols, J. Geophys. Res., 107, 4010, doi:4010.1029/2001JD000470, 2002a.
Kärcher, B. and Lohmann, U.: A parameterization of cirrus cloud formation: homogeneous freezing including effects or aerosol size, J. Geophys. Res., 107, 4698, doi:4610.1029/2001JD001429, 2002b.
Kärcher, B.: Simulating gas-aerosol-cirrus interactions: Process-oriented microphysical model and applications, Atmos. Chem. Phys., 3, 1645–1664, 2003, http://www.atmos-chem-phys.net/3/1645/2003/.
Kärcher, B. and Lohmann, U.: A parameterization of cirrus cloud formation: Heterogeneous freezing, J. Geophys. Res., 108, 4402, doi:10.1029/2002JD003220, 2003.
Kärcher, B., Hendricks, J., and Lohmann, U.: Physically based parameterization of cirrus cloud formation for use in global atmospheric models, J. Geophys. Res., 111, D01205, doi:01210.01029/02005JD006219, 2006.
Kärcher, B., Möhler, O., DeMott, P. J., Pechtl, S., and Yu, F.: Insights into the role of soot aerosols in cirrus cloud formation, Atmos. Chem. Phys., 7, 4203–4227, 2007, http://www.atmos-chem-phys.net/7/4203/2007/.
Kecs, W.: The convolution product and some applications, Mathematics and its applications, D.

Reidel co., Bucharest, Romania, 1982.
Khvorostyanov, V. I. and Curry, J. A.: The theory of ice nucleation by heterogeneous freezing of deliquescent mixed CCN. Part I: critical radius, energy and nucleation rate, J. Atmos. Sci., 61, 2676–2691, 2004.
Khvorostyanov, V. I. and Curry, J. A.: The theory of ice nucleation by heterogeneous freezing of deliquescent mixed CCN. Part II: parcel model simulations, J. Atmos. Sci., 62, 261–285, 2005.
Khvorostyanov, V. I. and Curry, J. A.: Critical humidities of homogeneous and heterogeneous ice nucleation: Inferences from extended classical nucleation theory, J. Geophys. Res., 114, D04207, doi:04210.01029/02008JD011197, 2009.
Koop, T., Luo, B., Tslas, A., and Peter, T.: Water activity as the determinant for homogeneous ice nucleation in aqueous solutions, Nature, 406, 611–614, 2000.
Lau, K. M. and Wu, H. T.: Warm rain processes over tropical oceans and climate implications, Geophys. Res. Lett., 30, 2290, doi:2210.1029/2003GL018567, 2003.
Lin, R., Starr, D., DeMott, P. J., Cotton, R., Sassen, K., Jensen, E. J., Kärcher, B., and Liu, X.: Cirrus parcel model comparison project. Phase 1: The critical components to simulate cirrus initiation explicitly, J. Atmos. Sci., 59, 2305–2328, 2002.
Linz, P.: Analytical and numerical methods for Volterra equations, SIAM studies in applied mathematics, SIAM, Philadelphia, PA, USA, 1985.
Liou, K.: Influence of cirrus clouds on weather and climate processes: a global perspective, Mon. Weather Rev., 114, 1167–1199, 1986.
Liu, X. and Penner, J. E.: Ice nucleation parameterization for global models, Meteorol. Z., 14, 499–514, 2005.
Marcolli, C., Gedamke, S., Peter, T., and Zobrist, B.: Efficiency of immersion mode ice nucleation on surrogates of mineral dust, Atmos. Chem. Phys., 7, 5081–5091, 2007, http://www.atmos-chem-phys.net/7/5081/2007/.
Meyers, M. P., DeMott, P. J., and Cotton, R.: New primary ice-nucleation parameterization in an explicit cloud model, J. Appl. Meteorol., 31, 708–721, 1992.
Minnis, P.: Contrails, cirrus trend, and climate, J. Climate, 17, 1671–1685, 2004.
Möhler, O., Büttner, S., Linke, C., Schnaiter, M., Saathoff, H., Stetzer, O., Wagner, R., Krämer, M., Mangold, A., Ebert, V., and Schurath, U.: Effect of sulfuric acid coating on heterogeneous ice nucleation by soot aerosol particles, J. Geophys. Res., 110, D11210, doi:11210.11029/12004JD005169, 2005.

Möhler, O., Field, P. R., Connolly, P., Benz, S., Saathoff, H., Schnaiter, M., Wagner, R., Cotton, R., Krämer, M., Mangold, A., and Heymsfield, A. J.: Efficiency of the deposition mode ice nucleation on mineral dust particles, Atmos. Chem. Phys., 6, 3007–3021, 2006, http://www.atmos-chem-phys.net/6/3007/2006/.

Monier, M., Wobrock, W., Gayet, J. F., and Flossman, A.: Development of a detailed microphysics cirrus model tracking aerosol particles histories for interpretation of the recent INCA campaign, J. Atmos. Sci., 63, 504–525, 2006.

Nenes, A. and Seinfeld, J. H.: Parameterization of cloud droplet formation in global climate models, J. Geophys. Res., 108, 4415, doi:4410.1029/2002JD002911, 2003.

Penner, J. E., Lister, D. H., Griggs, D. J., Dokken, D. J., and McFarland, M.: Aviation and the global atmosphere – A special report of IPCC working groups I and III. Intergovernmental Panel on Climate Change, Cambridge University Press, 365 pp., 1999.

Peter, T.: Microphysics and heterogeneous chemistry of polar stratospheric clouds Annu. Rev. Phys. Chem., 48, 785–822, 1997.

Phillips, V. T. J., Donner, L. J., and Garner, S. T.: Nucleation processes in deep convection simulated by a cloud-system-resolving model with double-moment bulk microphysics, J. Atmos. Sci., 64, 738–761, doi:710.1175/JAS3869.1171, 2007.

Phillips, V. T. J., DeMott, P. J., and Andronache, C.: An empirical parameterization of heterogeneous ice nucleation for multiple chemical species of aerosol, J. Atmos. Sci., 65, 2757–2783, doi:2710.1175/2007JAS2546.2751, 2008.

Prenni, A. J., DeMott, P. J., Twohy, C. H., Poellot, M. R., Kreidenweis, S. M., Rogers, D. C., Brooks, S. D., Richardson, M. S., and Heymsfield, A. J.: Examinations of ice formation processes in Florida cumuli using ice nuclei measurements of anvil ice crystal particle residues, J. Geophys. Res., 112, D10121, doi:10110.11029/12006JD007549, 2007.

Pruppacher, H. R. and Klett, J. D.: Microphysics of clouds and precipitation 2nd ed., Kluwer Academic Publishers, Boston, MA, 954 pp., 1997.

Ren, C. and Mackenzie, A. R.: Cirrus parameterization and the role of ice nuclei, Q. J. Roy. Meteor. Soc., 131, 1585–1605, doi:10.1256/qj.04.126, 2005.

Sassen, K., DeMott, P. J., Prospero, J. M., and Poellot, M. R.: Saharan dust storms and indirect aerosol effects on clouds: CRYSTAL-FACE results, Geophys. Res. Lett., 30, 1633, doi:1610.1029/2003GL017371, 2003.

Seinfeld, J. H.: Clouds, contrails and climate, Nature, 391, 837–838, 1998.

Tabazadeh, A., Jensen, E. J., and Toon, O. B.: A model description for cirrus cloud nucle-

ation from homogeneous freezing of sulfate aerosols, J. Geophys. Res., 102, 23485–23850, 1997a.

Tabazadeh, A., Toon, O. B., and Jensen, E. J.: Formation and implications of ice particle nucleation in the stratosphere, Geophys. Res. Lett., 24, 2007–2010, 1997b.

Vali, G.: Freezing rate due to heterogeneous nucleation, J. Atmos. Sci., 51, 1843–1856, 1994.

Vali, G.: Repeatability and randomness in heterogeneous freezing nucleation, Atmos. Chem. Phys., 8, 5017–5031, 2008, http://www.atmos-chem-phys.net/8/5017/2008/.

Waliser, D. E., Li, J. F., Woods, C. P., Austin, R. T., Bacmeister, J., Chern, J., Del Genio, A. D., Jiang, J. H., Kuang, Z., Meng, H., Minnis, P., Platnick, S., Rossow, W. B., Stephens, G. L., Sun-Mack, S., Tao, W., Tompkins, A. M., Vane, D. G., Walker, C., and Wu, D.: Cloud ice: A climate model challenge with signs and expectations of progress, J. Geophys. Res., 114, doi:10.1029/2008JD10015, 2009.

Welti, A., Lüönd, F., Stetzer, O., and Lohmann, U.: influence of particle size on the ice nucleating ability of mineral dusts, Atmos. Chem. Phys. Discuss., 9, 6929–6955, 2009, http://www.atmos-chem-phys-discuss.net/9/6929/2009/.

Zobrist, B., Koop, T., Luo, B., Marcolli, C., and Peter, T.: Heterogeneous ice nucleation rate coefficient of water droplets coated by a nonadecanol monolayer, J. Phys. Chem. C, 111, 2149–2155, 2007.

Zobrist, B., Marcolli, C., Peter, T., and Koop, T.: Heterogeneous ice nucleation in aqueous solutions: the role of water activity, J. Phys. Chem. A, 112, 3965–3975, 2008.

Zuberi, B., Bertram, A. K., Cassa, C. A., Molina, L. T., and Molina, M. J.: Heterogeneous nucleation of ice in $(NH_4)_2SO_4$-H_2O particles with mineral dust immersions, Geophys. Res. Lett., 29, 1504, doi:1510.1029/2001GL014289, 2002.

Table 1. Cumulative freezing spectra considered in this study. The functions $H_{soot}(s_i, T)$ and $H_{dust}(s_i, T)$ for PDA08 are defined in Phillips et al. (2008).

Spectrum	$N_{het}(s_i)$ (m^{-3})
Meyers et al. (1992), MY92	$10^3 e^{-0.639+12.96 s_i}$
Phillips et al. (2007), PDG07	$60 e^{-0.639+12.96 s_i} \quad 243 < T < 268$ $10^3 e^{-0.388+3.88 s_i} \quad 190 < T \leq 243$
Phillips et al. (2008), PDA08	$N_{dust}\left[1 - \exp\left(\frac{2}{3} H_{dust}(s_i, T) \frac{N_{het,PDG07}}{7.92 \times 10^4}\right)\right]$ $+ N_{soot}\left[1 - \exp\left(\frac{1}{3} H_{soot}(s_i, T) \frac{N_{het,PDG07}}{1.04 \times 10^6}\right)\right]$
Classical Nucleation Theory (Sect. 2.2), CNT	$0.05\left[\min\left(\frac{s_i}{0.2} N_{dust} e^{-0.0011 k_{hom}(0.2 - s_i)}, N_{dust}\right) + \min\left(\frac{s_i}{0.3} N_{soot} e^{-0.039 k_{hom}(0.3 - s_i)}, N_{soot}\right)\right]$

ACPD
9, 10957–11004, 2009

Table 2. Cloud formation conditions and aerosol characteristic used in the parameterization evaluation.

Property	Values
T_o(K)	205–250
V (m s^{-1})	0.04–2
α_d	0.1, 1.0
$\sigma_{g,dry}$	2.3
N_o (cm^{-3})	200
$D_{g,\mathrm{dry}}$ (nm)	40
N_{dust} (cm^{-3})	0.05–5
N_{soot} (cm^{-3})	0.05–5

ACPD
9, 10957–11004, 2009

Table 3. Average % relative error (standard deviation) of parameterized N_c and $s_{\max}$ against parcel model simulations. Results are shown for (a) heterogeneous freezing is only active, and, (b) homogeneous and heterogeneous nucleation are active. $N_{c,n}$,$N_{c,p}$, are ice crystal concentrations from parcel model and parameterization, respectively; similarly for maximum supersaturation, $s_{\max,n}$, $s_{\max,p}$.

Ice Formation Mechanism	Pure Heterogeneous		Homogeneous and Heterogeneous
Spectrum	$\frac{s_{\max,p}-s_{\max,n}}{s_{\max,n}}$	$\frac{N_{c,p}-N_{c,n}}{N_{c,n}}$	$\frac{N_{c,p}-N_{c,n}}{N_{c,n}}$
MY92	0.43(2.29)	1.14(13.3)	2.95(21.2)
PDG07	0.63(1.56)	3.39(7.60)	−3.78(20.7)
PDA08	−2.69(2.81)	−3.26(8.32)	9.64(21.1)
CNT	−0.44(5.56)	−1.56(4.14)	3.26(22.6)
All combined	−1.68(3.42)	−2.08(8.58)	4.72(21.8)

ACPD
9, 10957–11004, 2009

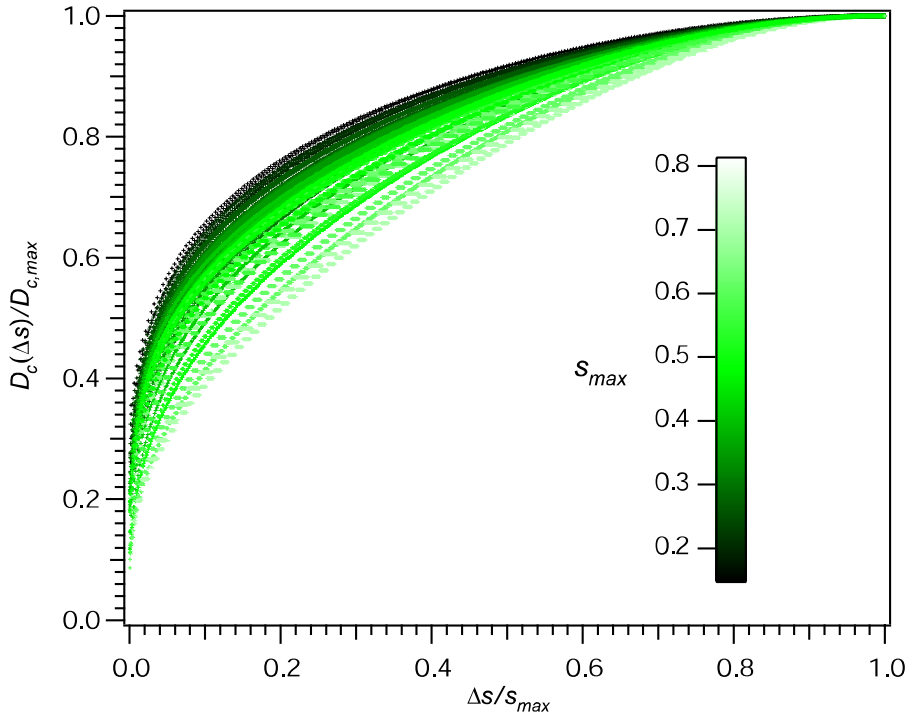

Fig. 1. $\frac{D_c(\Delta s)}{D_{c,\max}}$ vs. $\frac{\Delta s}{s_{\max}}$ for pure heterogeneous freezing and simulation conditions of Table 2 using the MY92 freezing spectrum.

ACPD
9, 10957–11004, 2009

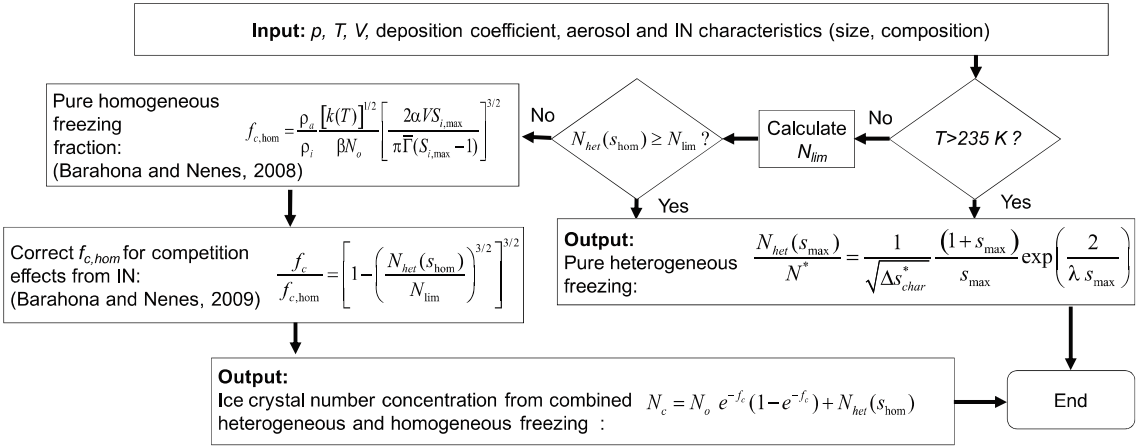

Fig. 2. Parameterization algorithm.

ACPD
9, 10957–11004, 2009

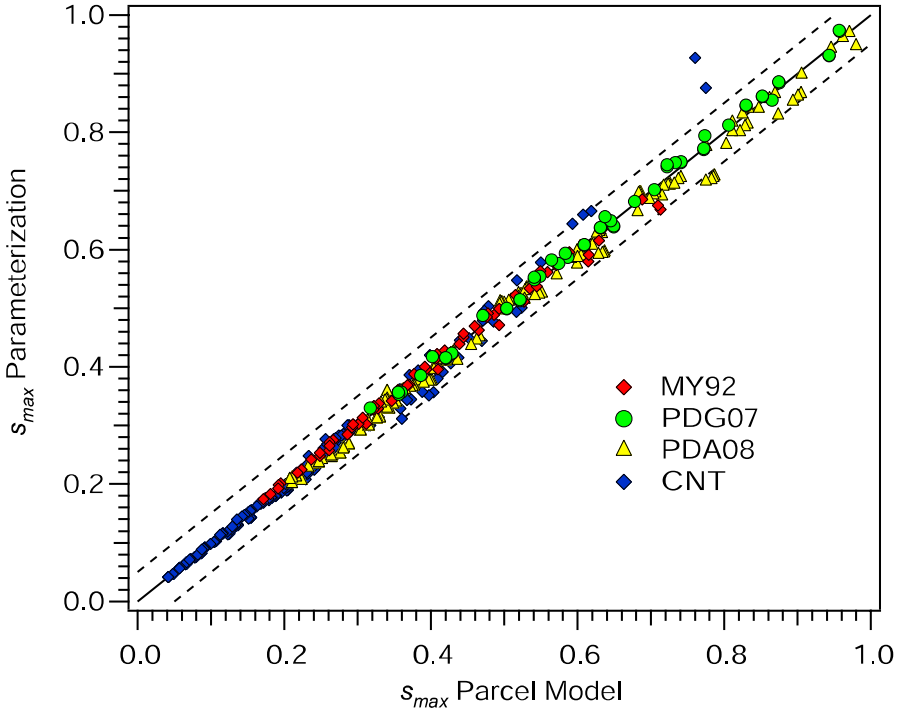

Fig. 3. Comparison between s_{max} predicted by parameterization and parcel model for conditions of pure heterogeneous freezing. Dashed lines represent the ±5% difference.

ACPD
9, 10957–11004, 2009

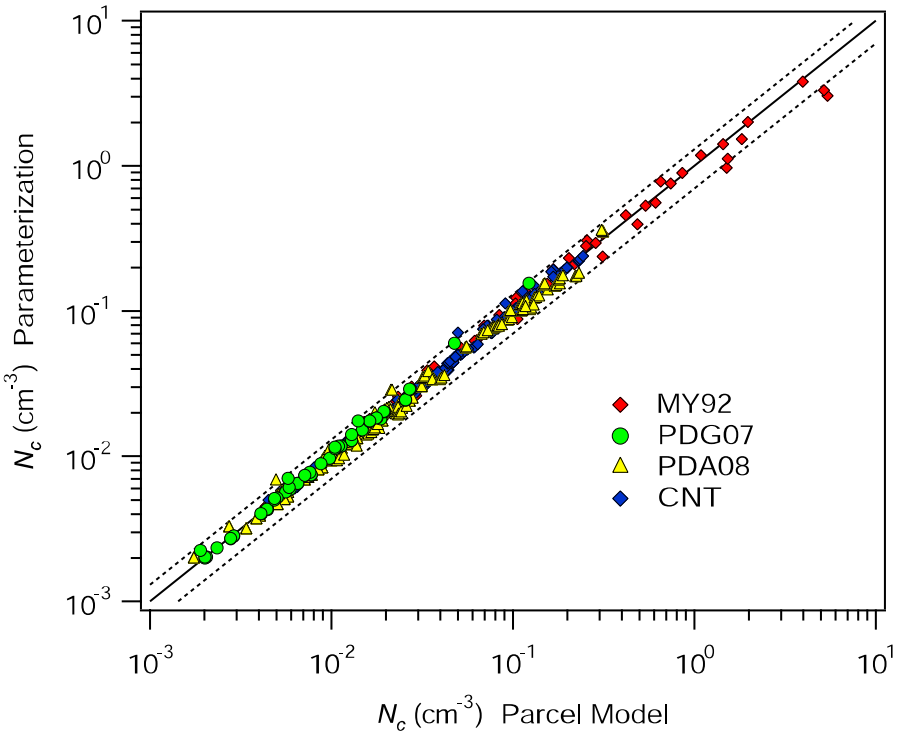

Fig. 4. Comparison between N_{het} from pure heterogeneous freezing predicted by the parameterization and the parcel model for simulation conditions of Table 2 and freezing spectra of Table 1. Dashed lines represent the ±30% difference.

ACPD
9, 10957–11004, 2009

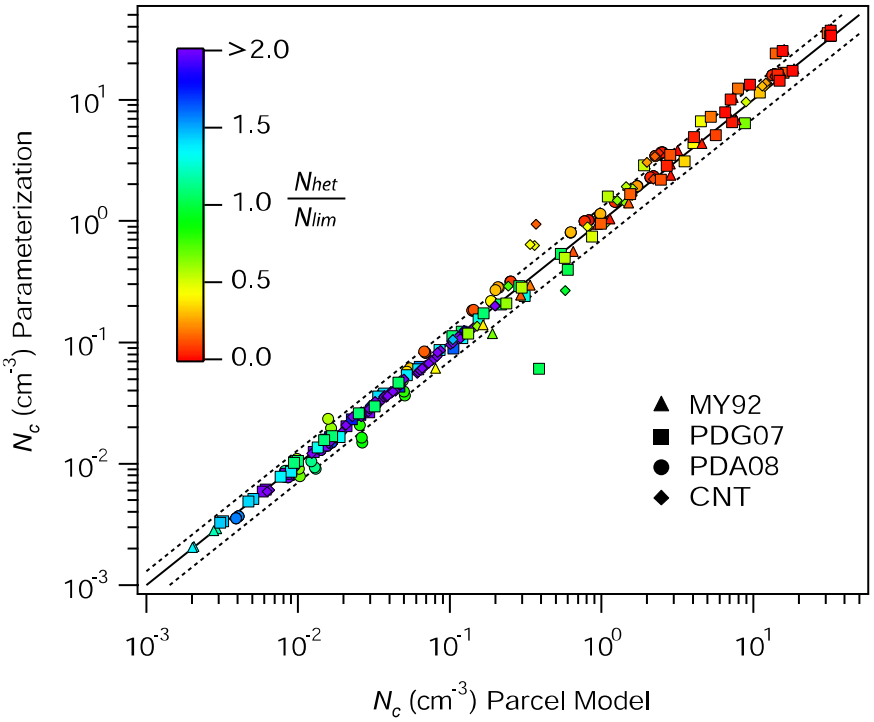

Fig. 5. Comparison between N_c from combined homogeneous and heterogeneous freezing predicted by the parameterization and the parcel model for simulation conditions of Table 2 and freezing spectra of Table 1. Dashed lines represent the ±30 % difference. Colors indicate the ratio $\frac{N_{het}}{N_{lim}}$.

ACPD
9, 10957–11004, 2009

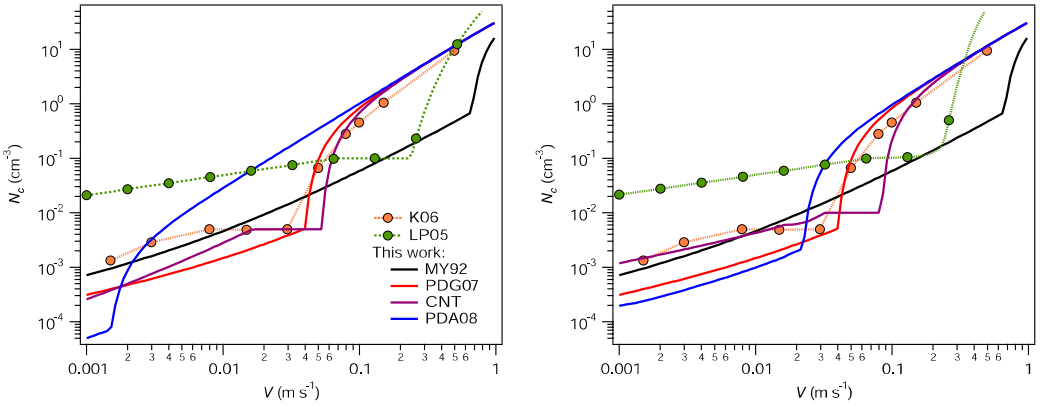

Fig. 6. N_c vs. V calculated using the new parameterization for all freezing spectra of Table 1. Also shown are results taken from Kärcher et al. (2006, K06) for $N_{IN}=5\times10^{-3}$ cm^{-3} and, the parameterization of Liu and Penner (2005). Conditions considered were $T_o=210$ K ($T=206$ K), $p=22000$ Pa, $\alpha_d=0.5$. Left panel: $N_{soot}=0.1$ cm^{-3}, $N_{dust}=0$ cm^{-3} and no deposition freezing considered in LP05. Right panel: $N_{soot}=0.1$ cm^{-3}, $N_{dust}=0.1$ cm^{-3} and deposition freezing considered in LP05.

ACPD
9, 10957–11004, 2009

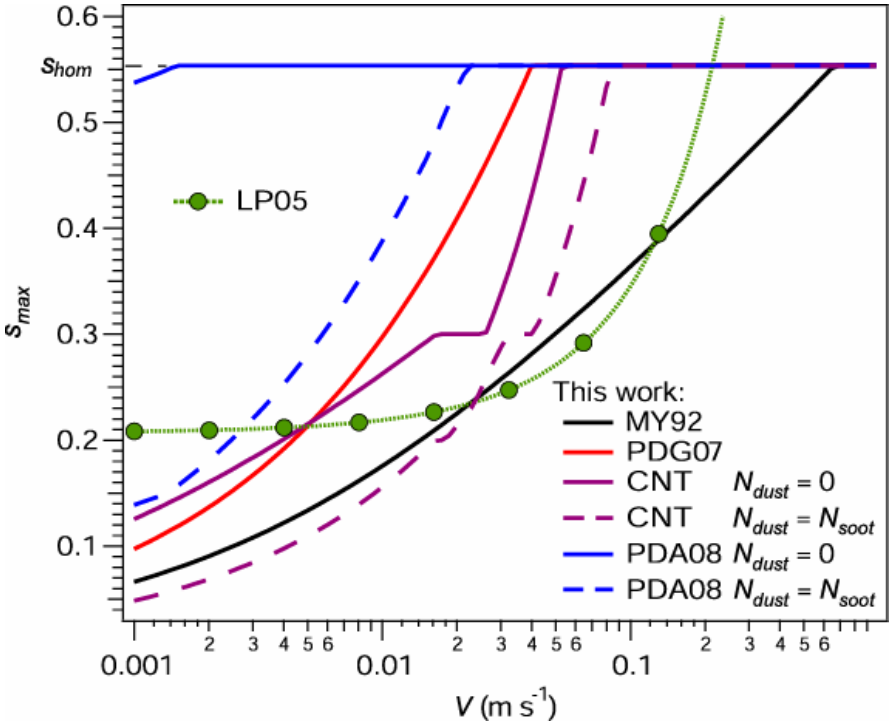

Fig. 7. s_{max} vs. V calculated using the parameterization of Liu and Penner (2005) and the new parameterization for all freezing spectra of Table 1 and conditions considered are similar to Fig. 6 and N_{soot} =0.1 cm^{-3}.

ACPD
9, 10957–11004, 2009